COVID Detection from X-RAY and CT Images Using Multiple Feature Extraction with Extreme Learning Machine and UNET

[1]V L NISHA, [2]D MENAKA

[1] Department of Electronics and Communication Engineering, Noorul Islam Centre for Higher Education, Kumaracoil, India
[2] Department of Electronics and Instrumentation Engineering, Noorul Islam Centre for Higher Education, Kumaracoil, India

Abstract: Coronaviruses are serious illnesses that affect both people and animals. Currently, the novel COVID-19 coronavirus is rapidly spreading over the world, putting billions of people's health. The majority of COVID-19 patients had a lung infection, according to clinical examinations. Computed Tomography (CT) is an effective imaging tool for identifying lung disorders which can have more detailed information about the chest region. Chest X-ray is more widely available due to its faster imaging time and lower cost. Deep learning, one of the most effective AI technologies, helps radiologists to analyze vast numbers of chest images, which is critical for rapid and reliable COVID-19 screening. The goal of this project is to create a new deep anomaly detection model that can be used quickly, reliable screening of COVID-19 from CT and X-Ray Images. Here, to create the segmentation map, UNET is used after training with the standard database of CT and X-ray images of COVID affected people. To classify normal, COVID or pneumonia, Extreme Learning Machine (ELM) is used with features such as centre symmetric local binary pattern (CSLBP), shape features and arithmetic features. To improve the performance, image denoising, smoothing, and normalization techniques are used in the pre-processing stage. To evaluate the performance, sensitivity, specificity, accuracy, and precision statistical measures were utilized. This work achieved a maximum accuracy of 98.93%. The results suggest that this work performs better than conventional covid classification works.

Keywords: *COVID-19, Pneumonia, Deep Learning, Image Smoothing, Extreme Learning Machine, UNET, Center Symmetric Local Binary Pattern (CSLBP), Shape Features, Arithmetic Features.*

1. INTRODUCTION

The new Coronavirus (COVID-19) is an acute, fatal disease that began in China's Wuhan province in December 2019 and has since expanded worldwide. Because no effective treatment has been established, the COVID-19 epidemic has been of significant worry to the medical world. COVID-19's biologic architecture is a positive-oriented single-stranded RNA-type, and the condition is difficult to treat owing to its mutating nature. Medical professionals throughout the globe are working hard to develop an appropriate cure for the condition. COVID-19 is the leading cause of mortality in the world today, with big outbreaks worldwide. Coronaviruses come in a variety of forms, and they're typically seen in animals. People with compromised immune systems may die as a result of the infection. COVID-19 is spread mostly through personal contact between people [1].

Artificial intelligence (AI) has recently been increasingly employed to speed up biological research. AI has been applied in a variety of applications, including picture detection, data categorization, and image segmentation, using deep learning methodologies. People who are infected with COVID-19 may get pneumonia as a result of the virus's ability to move to the lungs. Many deep learning projects have employed chest X-ray image data to identify the condition, and the results have been promising. [2].

When CT scans or X-Rays are used to identify COVID-19 symptoms in the lower lungs, the accuracy is greater than when RT-PCR is used. In certain cases, RT-PCR tests may take the role of CT scans and X-ray investigations. They are unable to adequately address the issue owing to the relatively limited number of radiologists compared to new

residents, as well as the high incidence of re-examinations of ill people who want to know how their health is going. The procedure's speed must be enhanced to accommodate the limits of CT scans and X-rays while also benefiting radiologists. Artificial intelligence (AI) tools may be integrated into contemporary diagnostic systems to do this. The objective is to reduce the time and effort required to do CT scans and X-rays on COVID-19-positive patients, as well as to measure the rate of disease progression [3].

Deep Learning approaches have exploded in popularity in recent years, drastically altering the landscape of numerous academic disciplines. When deep learning algorithms are utilized on image data sets including retina pictures, chest X-rays, and brain MRI, they produce promising results with a higher accuracy percent. X-ray machines are commonly used in hospitals to scan various human organs and provide more inexpensive and faster results. The manual interpretation of diverse X-ray images is usually performed by a trained radiologist. If you train those collected images using deep learning as a data scientist, you may greatly assist medical specialists in spotting COVID-19 patients. This should benefit underdeveloped nations where an X-ray facility is accessible but an expert is still a pipe dream [4].

There has been a slew of accomplishments in COVID-19 detection since the deep convolution neural network technology attained an extraordinary edge in image processing. The CXRadiographs probable imaging biomarkers and built a deep neural network for COVID-19 CXR image interpretation using a patch-based CNN technique with a minimal number of trainable parameters and few training data [5].

This work proposes a new technique to improve the accuracy of COVID detection using multiple feature extraction followed by feature position and weight optimization to increase the classification accuracy. The following features are extracted: CSLBP, Arithmetic function, and Shape feature, followed by the training and testing phase. Finally, the dataset is evaluated for performance, accuracy, sensitivity, specificity, precision, and kappa.

The remainder of the paper is laid out as follows: The experimental details are presented in Section 2. In Section 3, experimental results are discussed and analysed. Section 4, concludes the work.

2. DETAILS EXPERIMENTAL

2.1. Materials and Procedures

2.1.1 Dataset

The data collection utilised in this study is open source, and it presently has 337 pictures from 192 X-Ray scans of COVID-19 positive patients. Contributions are welcome to the photo archive, which is updated regularly with new images. All of the photos, as well as the X-ray results, have been inspected and commented on exhaustively. The images came from a variety of places, including Radiopedia.org., Kaggle image dataset. 1700 images were considered for classification. To classify these images, they were separated into three unique class values: Normal, Pneumonia, and Covid19. This data set is further divided into two parts: training and testing. The training portion contains 75% of the data for training the proposed deep learning model, while the testing portion contains 25% of the data for testing purposes.

2.1.2 Block diagram

Fig.1. shows COVID detection from CT images using multiple feature extraction with ELM. This work, consists of four framework components: Image preprocessing, segmentation, Feature extraction network training, and classification, also, data segmentation which plays an important role in this classification framework can be described and analyzed.

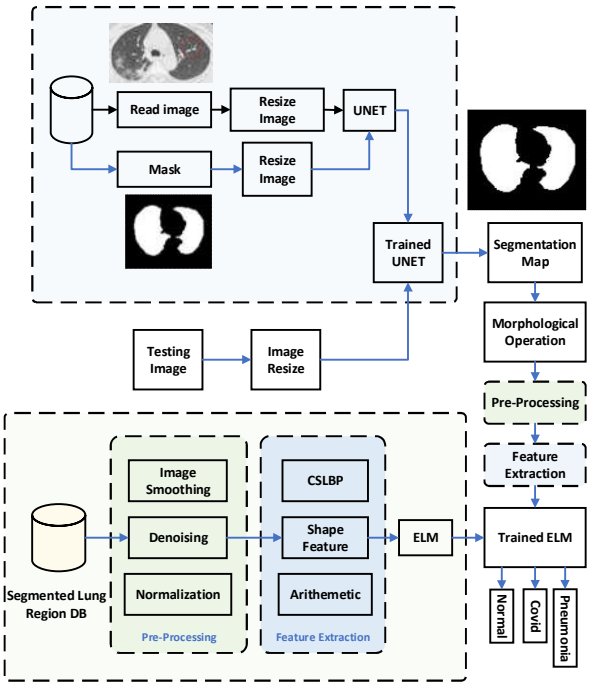

Fig.1. Block diagram for COVID detection using multiple feature extraction with ELM

2.1.3. UNET Architecture

The process of segmentation is accomplished by the use of an encoder-decoder neural network, commonly known as a UNET (unidirectional neural network). Performing a transposed convolution operation (deconvolution) on the information acquired in the decoder area of the network allows one to decode information from the latent space, therefore revealing previously hidden information. This model permits the simultaneous use of global location and context. and delivering outstanding segmentation performance.

As a consequence of the procedure, a picture segmentation mask is created for the image. Fig.2. depicts the UNET architecture.

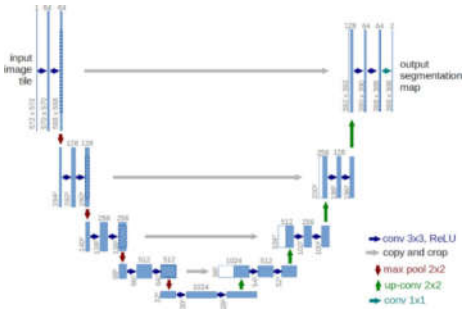

Fig.2 . UNET architecture

Except for the encoder section, the remaining phases are identical to those used in the encoder portion of the programme. While looking at these two frameworks, one of the primary distinctions is the use of skip-associations to move data from the suitable high-goal levels of the encoder to the relating high-goal layers of the decoder. Among UNET and the basic encoder-decoder worldview, which might empower the organization to better catch

minute subtleties that are available in high-goal. This organization's plan is partitioned into two segments: contractive and expansive. The contracting approach, which follows ReLU layers, consists of numerous convolution patches with size 3x3 filters and uni-ty strides in both directions. This route takes the most important properties from the input and returns a feature vector of a predetermined length.

The second route copies and crops data from the contractive path, as well as up-convolutions data from the feature vector, and then employs numerous techniques to build an output segmentation map. The UNET architecture is seen in Figure 2. The operation that connects the first and second pathways is a key feature of this system. This connection allows the network to get very precise data from the contractive route, resulting in a segmentation mask that is as near to the intended output as feasible.

2.1.4. Binary Dilation

In mathematical morphology, a binary image is considered a subset of a Euclidean space R^dor the integer grid Z^d for some dimension d. Assume E is a Euclidean space or an integer grid, A is a binary picture in E, and B is a structuring element that is a subset of R^d. The dilatation of A by B is calculated as follows:

$A \oplus B = \bigcup_{b \in B} A_b$ (1)

where $A_b$is the translation of A by b.

2.1.5. Feature Extraction

Using five independent feature selection techniques CSLBP, SIFT, SURF, and Arithmetic high-level features such as Standard Deviation(SD), mean, Kurtosis, skewness and moment with varying scales are retrieved from the segmented pulmonary areas in this stage. Because the retrieved attributes serve as the foundation for categorising the COVID-19, the classification approaches exhibited low classification accuracy. There is unanimity that no one function performs flawlessly since each feature has its own set of constraints.

2.1.6. Extreme Learning Machine (ELM)

The ELM is a unique learning algorithm for a feed-forward neural network with a single hidden layer (SLFN). The input weights and biases of ELM are selected at random in this technique, while the output weights are determined analytically. ELM has been used in several applications because of its exceptional generalisation performance and implementation efficiency. Weights of output are measured as shown in Eq.(4).

$f_L(x) = \sum_{i=1}^{L} \beta_i h_i(x) = h(x)\beta$ (4)

where $\beta = [\beta_1, ..., \beta_L]^T$ is the output weights vector between $h(x)$ is the output vector of the hidden layer, $h(x) = [G(a_1, b_1, x), \dots, G(a_L, b_L, x)]$ is $G(a, b, x)$ a nonlinear piecewise continuous function, $\{(a_i, b_i)\}_i^L = 1$ randomly generated input value.

$Sigmoid\ Function\colon\ G(a, b, x) = \frac{1}{1+exp(-(a.x+b))}$ (5)

From the input layer to the hidden layer, go through the following steps:, x is a sample of input, a is the value of the weight, and b is the value of bias. The $\{a, b\}$ pair is generated randomly. $\| H\beta - T \|^2$ and $\| \beta \|$ where H is the hidden layer output matrix;

$$\begin{bmatrix} h_1(x_1) & \dots & h_L(x_1) \\ \vdots & \ddots & \vdots \\ h_1(x_N) & \dots & h_L(x_N) \end{bmatrix}$$

During the application phase of ELM, the least-squares approach was utilised in place of the more traditional optimization methods.

$\beta = H^{\dagger}T,$ (6)

T is the tag matrix and $H^{\dagger}$ is the inverse of the hidden layer output matrix of Moore–Penrose generalized. $H = [h^{T}(x_1), \ldots, h^{T}(x_N)]^{T}$ N is the training sample used to acquire the results. The Moore–Penrose generalized latent layer output matrix inverse's function is to minimize the L2 norms in this case of $\| H\beta - T \|$ and $\| \beta \|$. A regularization coefficient C is included in an optimization approach used to improve the ELM's resilience and generalization capacity. Therefore, given a K kernel, the weight set is learned as:

$$\beta = \left(\frac{I}{C} + K\right)^{-1} T \qquad (7)$$

This job ends with the classifying step. In the classification procedure, there is a 10-fold cross validity. Fig.3. shows the ELM architecture

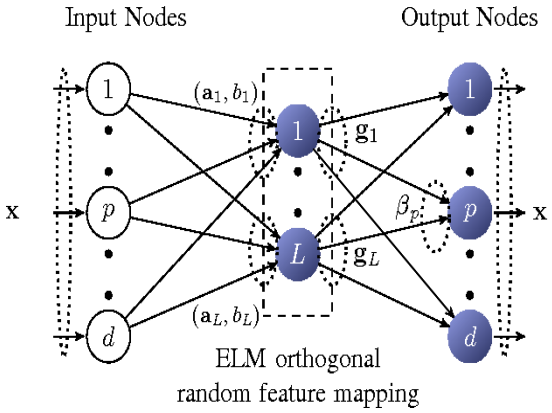

Fig.3. ELM architecture

3. RESULTS AND DISCUSSION

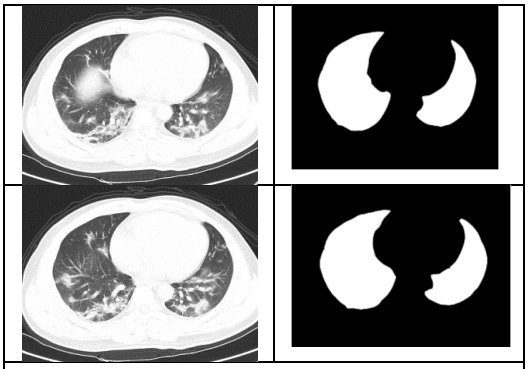

Fig.4.(a) Input CT image, Fig.4.(b) Segmentation map generated using UNET

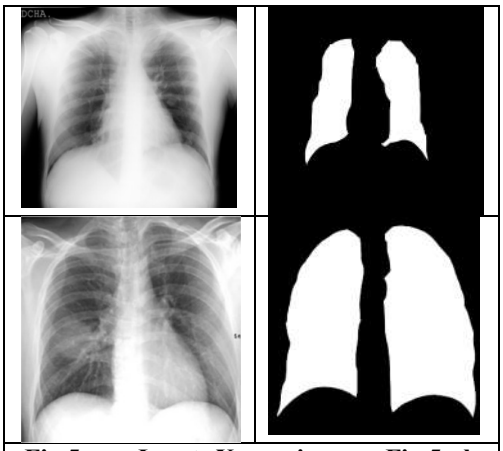

Fig.5. a. Input X-ray image, Fig.5. b. Segmentation map generated using UNET for X-ray image.

To evaluate the image classification using ELM, CT and X-ray images are collected from the Kaggle website. The average classification accuracy, which is the overall accurate classification score of all cell images utilized in the previous competition, is also determined for simplicity of comparison. MATLAB R2020b was used to complete this task using a machine with a Pentium(R) Dual-Core CPU E5800 @ 3.20GHz, 3192 MHz, 2 Core(s), and 2 GB of RAM.Fig.4. shows the segmentation performed by using UNET using CT images, Fig.5. shows the segmentation performed by using UNET for chest X-ray images.

3.2. Performance Analysis

Table.1 shows the training parameters of the proposed method. This method has 1000 of training images, 700 of testing images, 20 of epochs,50 of Iterations. Table.2 compares the performance of accuracy, sensitivity, and specificity on the Kaggle CT, X-ray dataset. It shows the highest performance displays when added X-RAY and CT images. The size of the image increased also decreases the accuracy. Table.3. displays comparison with previous methods. It shows this work produce 99.96 of accuracy, 98.2 of sensitivity, 99.53 of specificity, and 92.38 of precision. These results are highest result when compared to existing work. Table.4. displays the relative accuracy performance depending on the testing and training ratio. When taking 50% training and testing 34 images it has an accuracy of 62.3, sensitivity of 65.9, and specificity of 61.6. Suppose take 60% images for testing and 40% images for training to achieve 74.5 accuracies, 73.71 sensitivity, and 70.56 specificities. Finally get maximum accuracy of 96.1, a sensitivity of 96.4, and a specificity of 95.3 for applying 70% testing images and 25% training images. Table 5. Shows the training and Validation performance of Image segmentation (UNET) concerning iteration. Fig.6 shows the validation and training Accuracy concerning the number of iterations. Fig.7 shows the validation and training loss concerning the number of iterations.

Table.1 :Training Parameters of the proposed method

Number of training images	1000
Number of testing images	700
Number of epochs	20
Iterations	50

Table.2.: Performance of proposed method

Performance	X-ray	CT	X-Ray+CT
Accuracy	99.82	99.63	99.96
Sensitivity	98.2	98.46	98.41
Specificity	99.53	97.51	98.78
Precision	92.38	93.28	97.82

Table.3.Comparison with previous methods

Method	**Accuracy**	**Sensitivity**	**Specificity**	**Precision**
[7]	93	88	92	100
[10]	91.2	94.2	99.1	98.21
[11]	87.02	85.35	92.18	89.96
[12]	99.4	99.3	99.2	98.12
[13]	98.97	89.39	99.75	97.77
[14]	89.50	87.00	88.00	92.19
[15]	92.64	91.37	95.76	96.71
Proposed method	99.96	98.2	99.53	92.38

Table 4.: Comparative Performance Based on the Ratio of Testing and Training Images

	Percentage (%)		
Testing	50	60	75
Training	50	40	25
Accuracy	62.3	74.5	99.96
Sensitivity	65.9	73.71	96.4
Specificity	61.6	70.56	95.3

Table 5.:Training and Validation performance of Image segmentation (UNET) concerning iteration

No of Epochs	**TL**	**TA**	**VL**	**VA**
25	0.5217	96.5	0.5112	96.251
30	0.4631	97.1	0.4421	97.058
35	0.4123	97.5	0.3912	97.563
40	0.3621	98.6	0.3325	98.321
45	0.2516	99.1	0.2351	99.101
50	0.1475	99.6	0.1523	99.261

Fig.6. Validation and training Accuracy concerning the number of iterations

Fig.7. Validation and training loss concerning the number of iterations

3 CONCLUSION

In this work, a new technique is proposed to perform COVID-19 detection from CT and chest X-ray images. Initially, the segmentation map for the chest region is generated by using a trained UNET using a standard image database from the Kaggle website. The segmented chest region is further cropped and performed during the pre-processing operation. In the pre-processing, image denoising, smoothing, and resizing are performed to improve the quality of post-processing. Multiple features such as CSLBP, shape, and arithmetic features of the cropped region are extracted and trained using ELM for further prediction of Normal, Covid, or pneumonia classes. This work achieved a maximum accuracy of 99.96 % which is prior when compared to conventional covid classification techniques.

REFERENCES

1. Panwar, Harsh, P. K. Gupta, Mohammad Khubeb Siddiqui, Ruben Morales-Menendez, and Vaishnavi Singh. "Application of deep learning for fast detection of COVID-19 in X-Rays using nCOVnet." Chaos, Solitons & Fractals 138 (2020): 109944

2. Civit-Masot, Javier, Francisco Luna-Perejón, Manuel Domínguez Morales, and Anton Civit. "Deep learning system for COVID-19 diagnosis aid using X-ray pulmonary images." Applied Sciences 10, no. 13 (2020): 4640.

3. Jain, Rachna, Meenu Gupta, Soham Taneja, and D. Jude Hemanth. "Deep learning based detection and analysis of COVID-19 on chest X-ray images." Applied Intelligence 51, no. 3 (2021): 1690-1700.

4. Haque, Khandaker Foysal, and Ahmed Abdelgawad. "A deep learning approach to detect COVID-19 patients from chest X-ray images." AI 1, no. 3 (2020): 418-435.

5. Haghanifar, Arman, Mahdiyar Molahasani Majdabadi, Younhee Choi, S. Deivalakshmi, and Seokbum Ko. "Covid-cxnet: Detecting covid-19 in frontal chest x-ray images using deep learning." arXiv preprint arXiv:2006.13807 (2020).

6. Ismael, Aras M., and Abdulkadir Şengür. "Deep learning approaches for COVID-19 detection based on chest X-ray images." Expert Systems with Applications 164 (2021): 114054.

7. Zhou, Changjian, Jia Song, Sihan Zhou, Zhiyao Zhang, and Jinge Xing. "COVID-19 Detection based on Image Regrouping and ResNet-SVM using Chest X-ray Images." IEEE Access (2021).

8. Narin, Ali, Ceren Kaya, and Ziynet Pamuk. "Automatic detection of coronavirus disease (covid-19) using x-ray images and deep convolutional neural networks." Pattern Analysis and Applications (2021): 1-14.

9. Wang, Linda, Zhong Qiu Lin, and Alexander Wong. "Covid-net: A tailored deep convolutional neural network design for detection of covid-19 cases from chest x-ray images." Scientific Reports 10, no. 1 (2020): 1-12.

10. Hussain, Emtiaz, Mahmudul Hasan, Md Anisur Rahman, I ckjai Lee, Tasmi Tamanna, and Mohammad Zavid Parvez. "CoroDet: A deep learning-based classification for COVID-19 detection using chest X-ray images." Chaos, Solitons & Fractals 142 (2021): 110495.

11. Ismael, Aras M., and Abdulkadir Şengür. "The investigation of multiresolution approaches for chest X-ray image based COVID-19 detection." *Health Information Science and Systems* 8, no. 1 (2020): 1-11.

12. Haritha, D., M. Krishna Pranathi, and M. Reethika. "COVID detection from chest X-rays with DeepLearning: CheXNet." In *2020 5th International Conference on Computing, Communication and Security (ICCCS)*, pp. 1-5. IEEE, 2020.

13. Rai, Praveen, Ballamoole Krishna Kumar, Vijaya Kumar Deekshit, Indrani Karunasagar, and Iddya Karunasagar. "Detection technologies and recent developments in the diagnosis of COVID-19 infection." *Applied microbiology and biotechnology* 105, no. 2 (2021): 441-455.

14. Alwashmi, Meshari F. "The use of digital health in the detection and management of COVID-19." *International Journal of Environmental Research and Public Health* 17, no. 8 (2020): 2906.

15. Sethy, Prabira Kumar, and Santi Kumari Behera. "Detection of coronavirus disease (covid-19) based on deep features." (2020).

16. Ni, Ling, Fang Ye, Meng-Li Cheng, Yu Feng, Yong-Qiang Deng, Hui Zhao, Peng Wei et al. "Detection of SARS-CoV-2-specific humoral and cellular immunity in COVID-19 convalescent individuals." *Immunity* 52, no. 6 (2020): 971-977.